Fabrication of Alternating Multilayer Films of Graphene Oxide and Carbon Nanotube and Its Application in Mechanistic Study of Laser Desorption/Ionization of Small Molecules

Young-Kwan Kim[†] and Dal-Hee Min*[,‡]

[†]Department of Chemistry, Korea Advanced Institute of Science and Technology (KAIST), Daejeon, 305-701, Republic of Korea
[‡]Department of Chemistry, Seoul National University, Seoul, 151-747, Republic of Korea

Ⓢ Supporting Information

ABSTRACT: Graphene, graphene oxide (GO), and multi-walled carbon nanotube (MWCNT) have been actively explored as matrix for laser desorption/ionization mass spectrometry (LDI-MS) in place of conventional organic matrix. Recently, the GO/MWCNT double layer films on a solid substrate showed excellent applicability in small molecule analysis, enzyme activity assay and tissue imaging. In the present study, LDI processes of small molecules on multilayers of alternating MWCNT and GO hybrid films were thoroughly investigated. We found that the LDI efficiency of small molecules was affected by thickness, assembly sequence and surface roughness of the hybrid films that were controlled by varying the number of layer-by-layer (LBL) assembly cycles. The study would provide useful basic information to develop an efficient LDI-MS platform based on carbon nanomaterials.

Laser desorption/ionization
MWCNT-NH₂(GO/MWCNT-NH₂)ₙ multilayer

KEYWORDS: assembly, carbon nanotube, graphene, mass spectrometry, surface modification
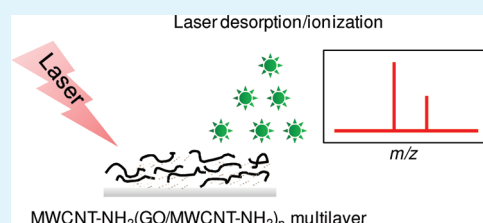
■ INTRODUCTION

Matrix-assisted laser desorption/ionization mass spectrometry (MALDI-MS) has been extensively harnessed as an important analytical tool for biochemical[1,2] and proteomic researches[3−5] because it could provide information on intact molecular weights of analytes.[6] Capability of soft-ionization of analytes without much fragmentation renders MALDI-MS attractive to analyze large biomolecules (1 to ~100 kDa) but the necessity of organic matrix molecules results in problems such as matrix ion interference in low-mass region,[7] sweet-spot formation,[8] and much trial-and-error to find the proper combination of matrix and analyte.[9] To solve the problems, researchers can employ laser desorption/ionization mass spectrometry (LDI-MS) without requiring organic matrix by using various nanostuctured surfaces such as porous silicon,[10−12] TiO_2,[13,14] silica,[15,16] and gold substrates.[17,18] In addition to the nanostructured surfaces, semiconductor[19−21] and metal[22−25] nanoparticles have been harnessed to facilitate LDI-MS analysis instead of conventional organic matrix. LDI-MS is especially efficient in analyzing small molecules with low molecular weights avoiding interference of peaks from organic matrix.

Recently, the carbon nanomaterials such as multi-walled carbon nanotube (MWCNT),[26−30] graphene[31−33] and graphene oxide (GO)[34] have been explored as an essential component of LDI-MS analysis since they absorb and transfer UV-laser energy to analyte. However, the direct application of the carbon nanomaterial suspensions in the form of mixed solutions with analytes showed drawbacks such as interference peaks in low-mass region of mass spectra and contamination of ionization source and detector induced by undesired ionization,

flight and fragmentation of carbon nanomaterials.[35] To address the problem, our group recently developed the surface-immobilized GO/MWCNT double-layer platform that showed excellent performance as a LDI-MS analysis platform for enzyme activity,[36] small molecules, and mouse brain tissue.[37]

Here, we prepared multilayers of alternating MWCNT and GO layers through layer-by-layer (LBL) assembly and systematically investigated the effect of number and sequence of the layers on LDI efficiency of small molecules. LBL assembly technique is useful to control the structures of nanohybrid films because the composition, thickness and surface properties can be controlled by changing the number and sequence of assembly cycles.[38,39] Therefore, LBL assembly technique has been employed in the fabrication of functional nanostructured films with appropriate surface functionalization for various applications such as drug delivery,[40,41] transparent electrodes,[42] electrochemical devices,[43] surface-enhanced Raman scattering (SERS)[44,45] and LDI-MS analysis.[46] In the present study, negatively charged GO[47] and positively charged MWCNT-NH₂[48] were harnessed for LBL assembly based on electrostatic interaction. The fabricated GO/MWCNT-NH₂ multilayer films with varying number of assembly cycles were thoroughly characterized and applied to LDI-MS analysis of various small molecules and mouse brain tissue slices (Scheme 1). The influence of GO/MWCNT-NH₂ multi-layer structures on LDI

Scheme 1. Scheme of Fabrication of MWCNT-NH$_2$/GO Multilayers by LBL Assembly and the Investigation of LDI-MS Efficiency of Small Molecules on the Prepared Multilayers
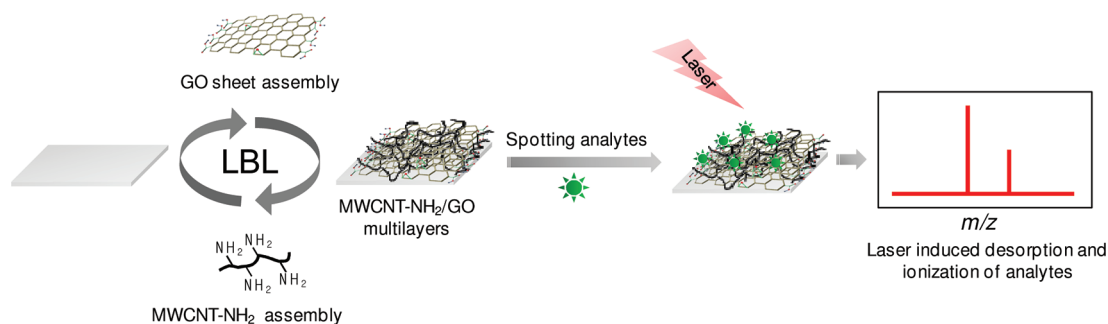
processes were discussed based on the characterization of the multi-layers and LDI-MS analysis results.

■ EXPERIMENTAL SECTION

Materials. Graphite (FP 99.95 % pure) was purchased from Graphit Kropfmühl AG (Hauzenberg, Germany). MWCNT (diameter in 15 nm and length 20 μm) was purchased from Nanolab (USA). Sodium nitrate and hydrogen peroxide (30 % in water) were purchased from Junsei (Japan). Cellobiose, Leu-enkephalin, glucose, lysine, leucine, phenylalanine, potassium permanganate, 3-amino-propyltriethoxysilane (APTES), 3-glycidylpropyltrimethoxysilane (GPTMS), ethylene diamine and anhydrous dimethylformamide (DMF) were purchased from Sigma-Aldrich (St. Louis, MO, USA). Nitric acid, sulfuric acid and thionyl chloride were purchased from Samchun (Seoul, Korea). Ethanol was purchased from Merck (Darmstadt, Germany). #2 glass coverslip (~0.22 mm in thickness), P^{++} Si substrates (500 μm in thickness) and 4 inch quartz wafers (500 μm in thickness) were purchased from Warner (Hamden, USA), STC (Japan) and i-Nexus (Stamford, USA), respectively. All chemicals were used without further purification.

Preparation of GPTMS-Functionalized Substrates. #2 glass coverslips were treated in Piranha solution (sulfuric acid: hydrogen peroxide (30 %) = 3:1, WARNING: Piranha solution is extremely explosive and corrosive.) for 10 min at 125 °C, washed with water and ethanol, and dried under a stream of nitrogen. The substrates were then immersed in a 10 mM anhydrous toluene solution of GPTMS for 30 min, rinsed with ethanol and water and dried under a stream of nitrogen. This process is applied to GPTMS functionalization of the used substrates such as Si and quartz substrates.

Preparation of MWCNT-NH$_2$(GO/MWCNT-NH$_2$)$_n$ Multilayer on Glass Substrate. The MWCNT-NH$_2$ and GO were prepared by previously reported methods (see the Supporting Information for the detailed procedure).[49,50] For immobilization of MWCNT-NH$_2$ with high surface coverage, the GPTMS-functionalized glass substrates were immersed in an aqueous MWCNT-NH$_2$ suspension (120 μg/mL) for 1 h, washed with water and ethanol, dried under a stream of nitrogen, and baked at 125 °C for 15 min under continuous nitrogen flow. The MWCNT-NH$_2$ coated substrates were employed as a substrate for subsequent, sequential LBL assembly of GO sheets and MWCNT-NH$_2$. The substrates were immersed in an aqueous GO suspension (1.5 mg/mL) for 1 h, washed with water and ethanol and dried under a stream of nitrogen. The above assembly processes were repeated until the desired number of MWCNT-NH$_2$(GO/MWCNT-NH$_2$)$_n$ multilayer was formed on the substrates. After finishing the multilayer fabrication, the substrates were baked at 150 °C for 15 min under continuous nitrogen flow.

Synthesis of Benzylpyridinium Salt (BP). 12 mL of pyridine was mixed with benzyl chloride at a molar ratio 20:1 (pyridine/benzyl chloride), refluxed at 60 °C for 6 h. The BP was collected by removal of excess pyridine with rotary evaporation under vacuum and used to prepare 1 mM methanolic solution.

LDI-MS Analysis of Small Molecules. The small molecules used in this study such as cellobiose, Leu-enkephalin, glucose, lysine, leucine and phenylalanine were dissolved in water at 1 nmol/μL by using vortex. 1 μL of the prepared small molecules solutions were deposited on the MWCNT-NH$_2$, MWCNT-NH$_2$/GO and MWCNT-NH$_2$(GO/MWCNT-NH$_2$)$_n$ multilayer-coated glass substrates, dried under ambient conditions, and mounted on the MTP TLC Adapter (Bruker Daltonics, Germany). The substrates mounted adapter was loaded into mass spectrometer and subjected to LDI-MS analysis under the constant experimental condition such as constant laser power and the number of laser shots using manual mode. This sample preparation process was applied to examining detection limit of small molecules in water and phosphate buffered saline (PBS) and monitoring LDI characteristics of BP as a thermometer molecule.

Preparation of the Mouse Brain Tissue Slice. After anesthetizing by i.p. injection of a mixture of ketamine and xylazine (4:1, 0.005 mg/g body weight), the mice (C57/BL6) were decapitated. After removing the skull, the brain was isolated and immersed in liquid nitrogen for 5 min. After the brain was frozen, brain slices were prepared with a thickness of 15 μm in the coronal direction at −25°C by using a cryotome (CM 1850, Leica, Nusslach, Germany), and immediately mounted on the MWCNT-NH$_2$(GO/MWCNT-NH$_2$)$_5$ film-coated substrates.

Characterization. The atomic force microscopy (AFM) images, line-profiles and center-line average surface roughness of the MWCNT-NH$_2$(GO/MWCNT-NH$_2$)$_n$ multilayer on silicon substrates were obtained with an XE-100 (Park System, Korea) with a backside gold-coated silicon SPM probe (M to N, Korea). All LDI-MS analyses of various molecules on MWCNT-NH$_2$(GO/MWCNT-NH$_2$)$_n$ multi-layer-coated glass substrates were carried out using a Bruker Autoflex III (Bruker Daltonics, Germany) equipped with a Smartbeam laser (Nd:YAG, 355 nm, 100 Hz, 50 μm of spot diameter at target plate) in positive reflection mode. The accelerating voltage was 19 kV and all spectra were obtained by averaging 500 laser shots. The UV-vis spectra of MWCNT-NH$_2$(GO/MWCNT-NH$_2$)$_n$ multilayer on quartz substrates were recorded with a UV-2550 (Shimadzu, Japan). Ellipsometric analysis was carried out with a L116S (Gaertner Scientific Corportation, USA). Raman characterization was carried out by LabRAM HR UV/vis/NIR (Horiba Jobin Yvon, France) using an Ar ion CW laser (514.5 nm) as an excitation source focused through a BXFM confocal microscope equipped with an objective (50×, numerical aperture = 0.50). FT-IR spectra measurements of graphite oxide were performed with an EQUINOX55 (Bruker, Germany) using the KBr pellet method.

■ RESULTS AND DISCUSSION

The GO and MWCNT-NH$_2$ were prepared by previously reported methods and dispersed in water by sonication to make each aqueous suspension (Figure S1a,b in the Supporting Information).[49,50] The MWCNT-NH$_2$ and GO presenting positive and negative charges, respectively, were used to fabricate the GO and MWCNT-NH$_2$ multilayers on glass coverslips by using LBL assembly based on electrostatic interaction.[51] First, the GO sheets were immobilized on
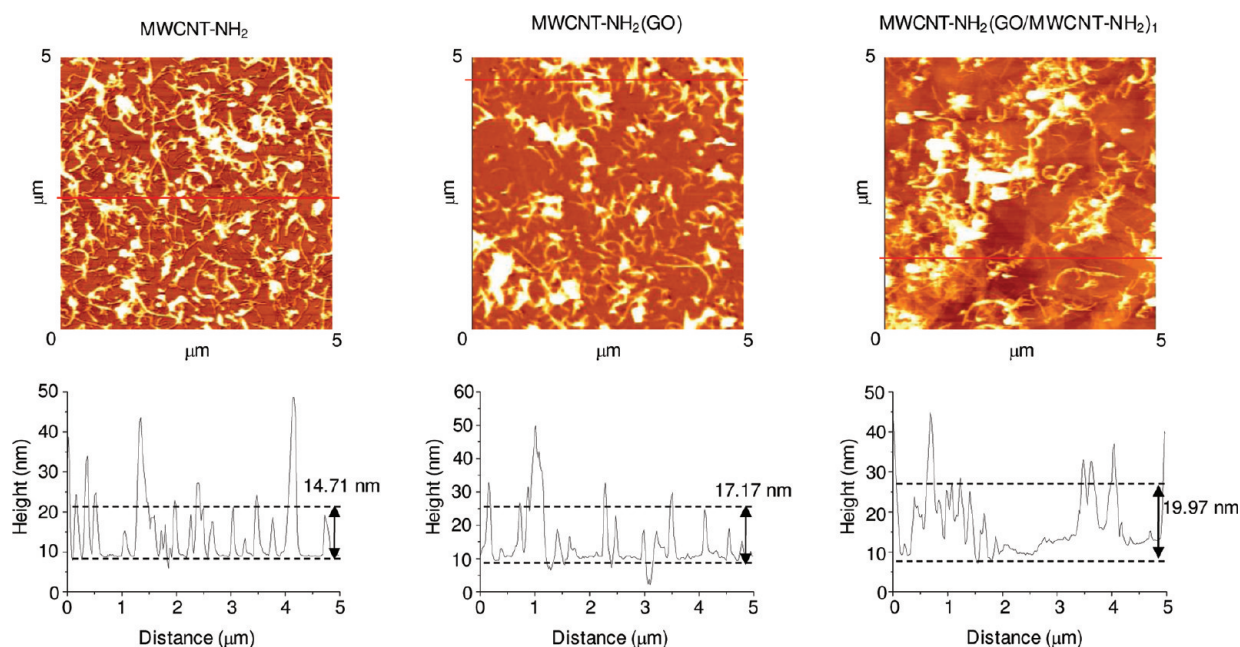
2089

dx.doi.org/10.1021/am300054z | ACS Appl. Mater. Interfaces 2012, 4, 2088−2095

Figure 1. AFM images and height profiles of MWCNT-NH$_2$, MWCNT-NH$_2$(GO) and MWCNT-NH$_2$(GO/MWCNT-NH$_2$)$_1$ coated-substrates. The height profile and aggregated domains of MWCNT-NH$_2$ films were increased by LBL assembly of GO sheets from 14.71 nm to 17.17 nm. Further assembly of MWCNT-NH$_2$ on the MWCNT-NH$_2$(GO) film resulted in the increased height profile to 19.97 nm with large aggregated domains.
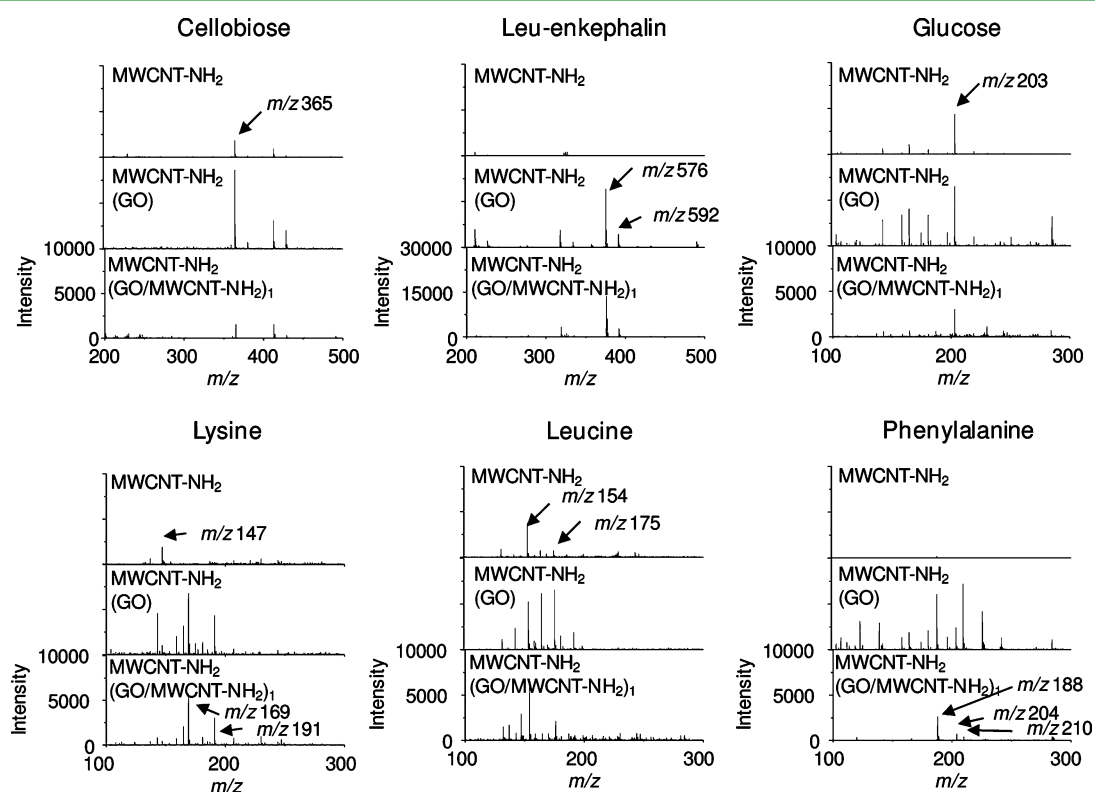

Figure 2. Mass spectra of various small molecules such as cellobiose, Leu-enkephalin, glucose, lysine, leucine, and phenylalanine obtained on MWCNT-NH$_2$, MWCNT-NH$_2$(GO), and MWCNT-NH$_2$(GO/MWCNT-NH$_2$)$_1$ film-coated substrates.

APTES treated glass substrate by immersing the substrate in GO suspension and the GO-coated surface was thermally treated to ensure robust binding.[51] This process resulted in the formation of uniform GO films with high surface coverage with average thickness of ~1−3 nm (Figure S1c). However, the fabricated GO film did not give sufficient peak intensities in

LDI-MS analysis of small molecules probably due to insufficient energy absorption and/or transfer from laser.[37] On the other hand, higher LDI efficiency of small molecules was obtained on the MWCNT-NH$_2$ film fabricated by immersing the GPTMS-treated glass substrate into MWCNT-NH$_2$ suspension
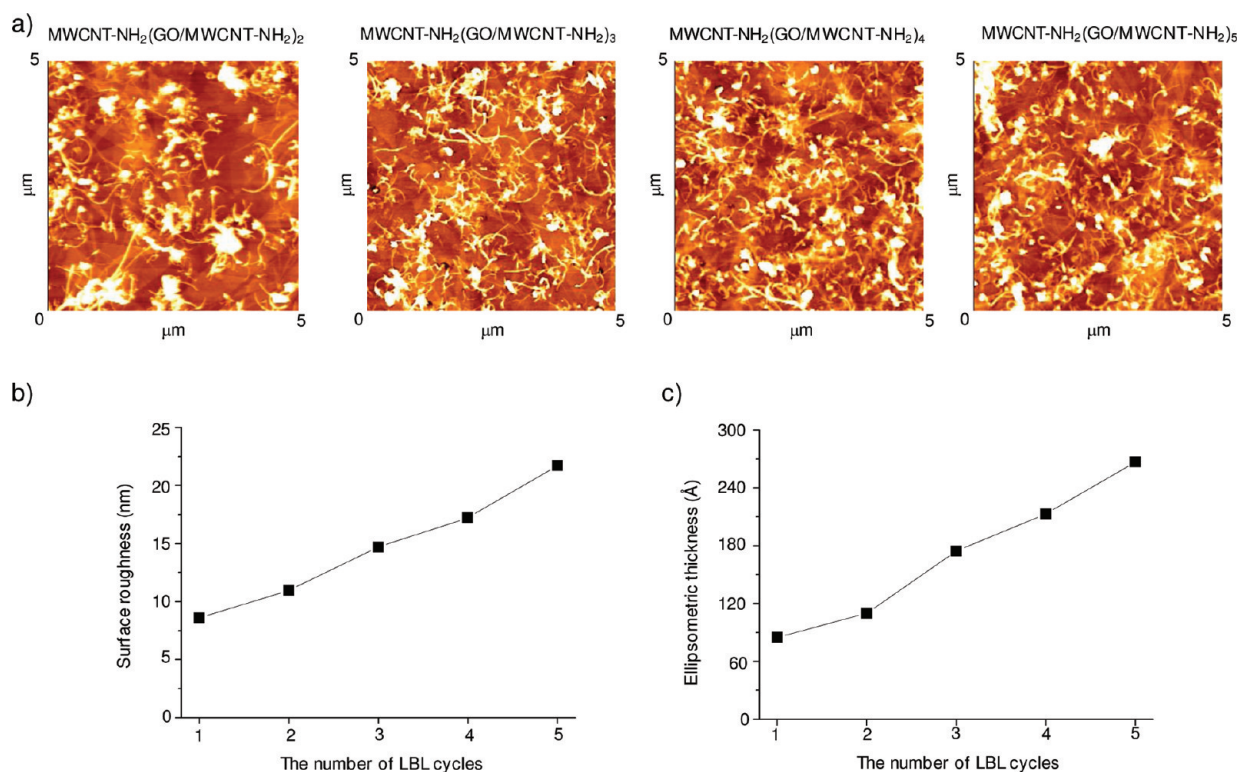
a)

b)

c)

Figure 3. (a) AFM images of MWCNT-NH$_2$(GO/MWCNT-NH$_2$)$_{2-5}$ multilayer showed the increased surface coverage and aggregated domains as each LBL assembly cycle was added. The CLA surface roughness (b) and ellipsometric thickness (c) were almost linearly increased with each LBL assembly cycle. These results well concurred with UV-vis analysis results (see Figure S3 in the Supporting Information).

compared to the GO film (Figure 2).[37] Therefore, MWCNT-NH$_2$ was chosen as a material for first layer.

We next fabricated MWCNT-NH$_2$/GO hybrid films via alternating assembly of the MWCNT-NH$_2$ and GO sheets on the MWCNT-NH$_2$ coated substrate. The MWCNT-NH$_2$(GO/MWCNT-NH$_2$)$_1$ multilayer was fabricated by sequential assembly of GO and MWCNT-NH$_2$ on the MWCNT-NH$_2$ film, where the subscript number indicates the number of LBL assembly cycles of GO sheet and MWCNT-NH$_2$. The fabricated GO and MWCNT-NH$_2$ hybrid films were characterized by AFM. On the MWCNT-NH$_2$ films, MWCNT-NH$_2$ was uniformly immobilized on the overall surface of substrates. By assembly of GO sheets on the MWCNT-NH$_2$ coated surface, MWCNT-NH$_2$ on substrates was decorated by GO sheets like sheath resulting in the increased number of aggregated domains and thickness from 14.71 to 17.17 nm. The resulting MWCNT-NH$_2$(GO) film was successively used as a substrate for followed LBL assembly of MWCNT-NH$_2$. The MWCNT-NH$_2$(GO/MWCNT-NH$_2$)$_1$ showed further increased film thickness from 17.17 to 19.97 nm (Figure 1). Next, 1 nmol of each small molecule (cellobiose, enkephaline, glucose, lysine, leucine and phenyl-alanine) was deposited on the prepared carbon nanomaterial hybrid films and subjected to LDI-MS analysis. On the MWCNT-NH$_2$ films, cellobioise, glucose, lysine, and leucine among the tested analytes were clearly detected as protonated ion and sodium adducts with little background interference (cellobiose: m/z 365 [M+Na]$^+$, glucose: m/z 203 [M+Na]$^+$, lysine: m/z 147 [M+H]$^+$, leucine : m/z 154 [M+H]$^+$ and m/z 175 [M+Na]$^+$). In contrast, after assembly of GO sheets on MWCNT-NH$_2$ films (MWCNT-NH$_2$(GO)), all analytes were detected with significantly increased mass peak intensities as

protonated ions and sodium and/or potassium adducts but background interference in low mass-region also increased significantly (cellobiose: m/z 365 [M+Na]$^+$, Leu-enkephalin: m/z 576 [M+Na]$^+$ and m/z 592 [M+K]$^+$, glucose: m/z 203 [M+Na]$^+$, lysine: m/z 169 [M+Na]$^+$ and m/z 191 [M+2Na]$^+$, leucine : m/z 154 [M+H]$^+$ and m/z 175 [M+Na]$^+$, and phenylalanine: m/z 188 [M+Na]$^+$, m/z 204 [M+K]$^+$ and m/z 210 [M+2Na]$^+$) (Figure 2). The cation adducts were frequently formed during LDI-MS analysis on carbon nano-materials such as carbon nanotube[26−30] and graphene[31−33] and origin of cations might be the residual Na$^+$ and K$^+$ ions on MWCNT-NH$_2$ and GO sheets from synthesis and immobiliza-tion processes. The high background interference might be attributed to the laser induced fragmentation of GO sheets due to the low thermal stability.[37] The background interference observed from MWCNT-NH$_2$(GO) films almost disappeared when the substrates were further coated with MWCNT-NH$_2$ on top of MWCNT-NH$_2$(GO) films with improved peak intensities. This result suggested that MWCNT-NH$_2$ is appropriate as a top surface material for efficient LDI-MS analysis of small molecules with little background interference probably because of relatively high thermal stability and energy absorption efficiency compared to GO sheets (see Figure S2 in the Supporting Information).

To investigate the relationship of the thickness and center-line average (CLA) surface roughness of MWCNT-NH$_2$(GO/MWCNT-NH$_2$)$_n$ multilayers with LDI efficiency of small molecules, the MWCNT-NH$_2$(GO/MWCNT-NH$_2$)$_n$ multi-layers were fabricated by alternating immersion of MWCNT-NH$_2$ coated substrates in GO and MWCNT-NH$_2$ suspensions. The growth of MWCNT-NH$_2$(GO/MWCNT-NH$_2$)$_n$ multi-layers on quartz substrates was monitored with a UV-vis
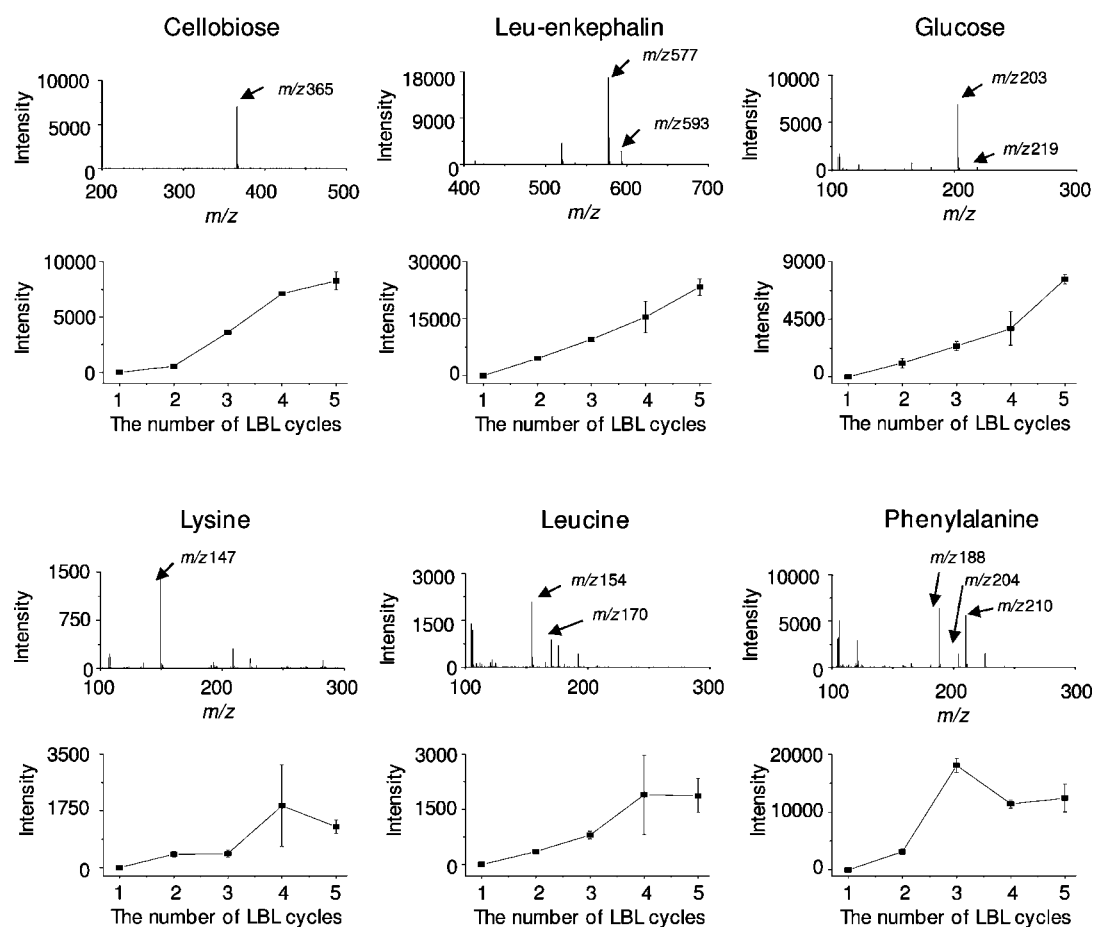
Figure 4. Mass spectra of various small molecules—cellobiose, Leu-enkephalin, glucose, lysine, leucine and phenylalanine—obtained on MWCNT-$NH_2(GO/MWCNT-NH_2)_5$ multilayer-coated substrates. Plots of average mass signal intensities of each small molecule versus number of LBL assembly cycle were also presented.

spectrophotometer. The absorbance of the MWCNT-$NH_2(GO/MWCNT-NH_2)_n$ multilayers at 263 and 355 nm almost linearly increased as LBL assembly cycle increased up to five (see Figure S3 in the Supporting Information). This result well matched with the linearly increased ellipsometric thickness of MWCNT-$NH_2(GO/MWCNT-NH_2)_{1-5}$ multilayers from 8.4 ($n = 1$) to 26.7 nm (n=5) with increasing assembly cycles on silicon substrates (Figure 3c). The results indicated that MWCNT-$NH_2(GO/MWCNT-NH_2)_n$ multilayers can be assembled with linear increase within a range of 1-5 LBL assembly cycles. However, the linearity could not be further applied to the films assembled with more than 5 LBL cycles, which we therefore excluded in the present study. Next, surface morphology and CLA surface roughness of MWCNT-$NH_2(GO/MWCNT-NH_2)_{1-5}$ multilayers were characterized by using AFM. The surface coverage of MWCNT-$NH_2(GO/MWCNT-NH_2)_n$ increased by the repeated LBL assembly cycles of GO and MWCNT-NH_2 but the morphologies were not significantly changed during 5 LBL assembly cycles. By contrast, the CLA surface roughness of MWCNT-$NH_2(GO/MWCNT-NH_2)_1$ multilayer gradually increased from 8.6 ($n = 1$) to 21.7 nm ($n = 5$) as the number of LBL assembly cycles increased (Figure 3a,b).

Next, 1 nmol of small molecules was deposited on the MWCNT-$NH_2(GO/MWCNT-NH_2)_{1-5}$ multilayer-coated glass substrates and subjected to LDI-MS analysis. The mass peak corresponding to each analyte was intensified as the assembly

of GO sheets and MWCNT-NH_2 repeated up to 5 cycles without significant background interference (Figure 4). The enhancement of mass peak intensity could be attributed to the enhanced absorption of excitation laser energy (wavelength at 355 nm) employed in LDI-MS analysis. For quantitative comparison, the detection limit of small molecules was next obtained on the MWCNT-$NH_2(GO/MWCNT-NH_2)_5$ multilayer. The detection limits were determined as 10 pmol for cellobiose, Leu-enkephalin and phenyl alanine, and 100 pmol for glucose, lysine and leucine in distilled water and the values increased by one order of magnitude in PBS (see Figures S4 and S5 in the Supporting Information). The both detection limits in water and PBS were lower than those obtained on previously reported GO/MWCNT-NH_2 double layer platform by one order of magnitude.[37] We think that the detection limit of small molecules on the MWCNT-$NH_2(GO/MWCNT-NH_2)_5$ multilayer is better than that on the GO/MWCNT-NH_2 double layer because of higher laser absorption that is strongly related to the thickness and the roughness of surfaces, which are known as important surface properties to be considered for fabricating efficient LDI-MS platform.[46] On the basis of the results, the influence of thickness and surface roughness of MWCNT-NH_2 and GO hybrid films on LDI efficiency of small molecules could be systematically investigated.

Next, we employed benzylpyridinium salt (BP) as a model analyte to determine two parameters—survival yield and desorption efficiency that estimate how well the generated
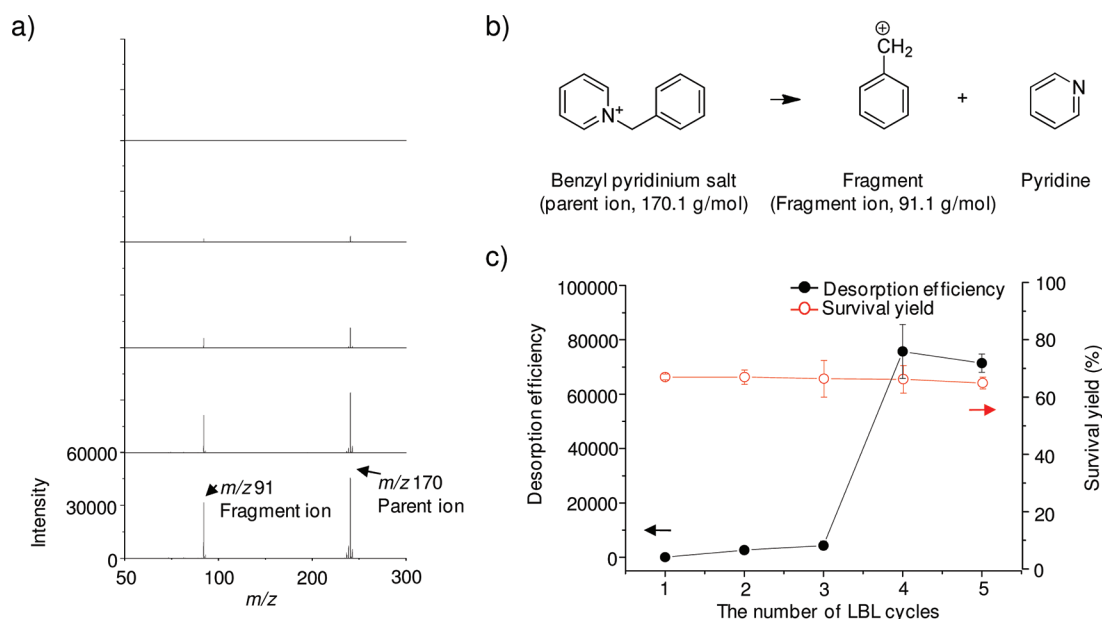
Figure 5. (a) Mass spectra of BP obtained on MWCNT-NH$_2$(GO/MWCNT-NH$_2$)$_{1-5}$ multilayer-coated substrates. (b) The fragmentation of BP during LDI-MS experiment. (c) The changes of average survival yield and desorption efficiency of BP on the MWCNT-NH$_2$(GO/MWCNT-NH$_2$)$_{1-5}$ multilayer-coated substrates. The average survival yield gradually decreased but desorption efficiency greatly increased with each LBL assembly cycle.
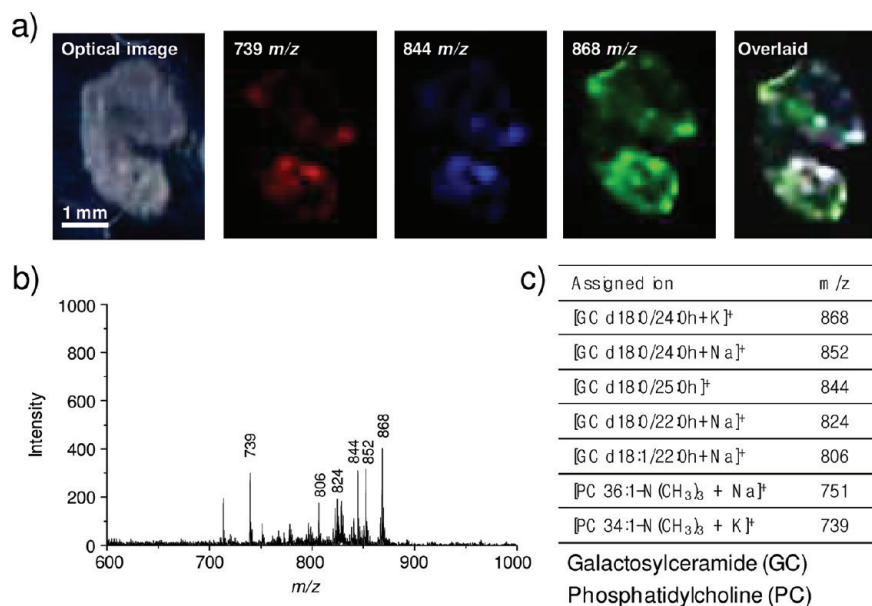

Figure 6. (a) Optical and mass images of a mouse brain tissue slice on a MWCNT-NH$_2$(GO/MWCNT-NH$_2$)$_5$ film coated substrate. (b) Accumulated mass spectrum from the mouse brain tissue slice. (c) Table of the ionized species identified in the mass spectrum.

intact molecular ions survive avoiding fragmentation under the given condition and how efficiently the analytes are desorbed from the given substrate, respectively.[52] It is well-known that high desorption efficiency and survival yield are favored for the development of good LDI system. In our system, survival yield and desorption efficiency were calculated by averaging at least 3 mass spectra of BP obtained with MWCNT-NH$_2$(GO/MWCNT-NH$_2$)$_n$ multilayers, by dividing the peak intensity of the parent ion by the total mass peak intensities of the fragment and parent ions, and by summing the absolute intensities of the fragment and parent ions, respectively. The average survival yield and desorption efficiency of BP were determined as 67% and 30 on MWCNT-NH$_2$ film. The average

survival yield gradually decreased to 64% but desorption efficiency greatly increased up to 71381 as LBL assembly cycles of GO and MWCNT-NH$_2$ were added up to 5 cycles (Figure 5). The results indicated that the relatively high desorption efficiency from the increased laser absorption of MWCNT-NH$_2$(GO/MWCNT-NH$_2$)$_5$ multilayer lead to enhancement of LDI efficiency to give low detection limit by providing adequate laser energy absorption and transfer to analytes but this favorable effect was slightly countervailed by the small decrease in the survival yield from 67 to 64%, probably because of overheating.

Finally, the MWCNT-NH$_2$(GO/MWCNT-NH$_2$)$_5$ film-coated substrates were applied to imaging mass spectrometry

(IMS) of lipids that were distributed in a mouse brain tissue slice.[37] The precise imaging of lipid distribution and their identification are urgent issues because lipid is one of the essential biomolecules in the most of important biological processes.[53] For the IMS analysis, mouse brain tissue sections (15μm in thickness) were prepared by saggital cutting, placed side by side on the top surface of the MWCNT-NH$_2$(GO/ MWCNT-NH$_2$)$_5$ film-coated substrates, directly analyzed by using a laser beam diameter of 50 μm at the target plate and raster width of 100 μm (Figure 6). Several phosphatidylcholine (PC) and glycerophosphocholine (GC) derivatives were successfully detected as sodium and potassium adducts (Figure 6c) in the tissue slice with the distributions comparable to previous reports.[37] A total ionized species was mapped with the mass peaks corresponding to [PC 34:1-N(CH$_3$)$_3$ + K]$^+$, [GC d18:0/24:0h+K]$^+$ and [GC d18:1/22:0h+Na]$^+$ (Figure 6a). This IMS result confirmed that the present MWCNT-NH$_2$(GO/MWCNT-NH$_2$)$_5$ films coated substrates is a promising platform for direct IMS analysis of tissue section without the disadvantages associated with conventional organic matrix, such as formation of inhomogeneous signal acquisition and sublimation during the lengthy IMS analysis.

CONCLUSION

In conclusion, we investigated the structural factors of alternating GO and MWCNT-NH$_2$ hybrid multilayers on the LDI-MS efficiency of small molecules and tissue slices. The structural factors such as thickness and CLA surface roughness of MWCNT-NH$_2$(GO/MWCNT-NH$_2$)$_n$ multilayer were successfully controlled by LBL assembly and its optical and physical properties were thoroughly characterized to comprehensively elucidate the correlation between structural factors and LDI efficiency of MWCNT-NH$_2$(GO/MWCNT-NH$_2$)$_n$ multilayer. On the basis of the results, we found that (i) the optimal number of layers is five, (ii) MWCNT-NH$_2$, not GO, should be present at the very top surface for better performance, and (iii) the relationship of surface characteristics with survival yield and desorption efficiency. We believe that the present study can serve as meaningful and important basis for the development of efficient LDI-MS analysis platform by using carbon nanomaterials. We are currently developing LDI-MS platforms based on carbon nanomaterials optimized for specific samples, for example, oligosaccharides, hydrophobic molecules, and peptides, for various bioanalytical applications.

ASSOCIATED CONTENT

Ⓢ Supporting Information

Analytical data. This material is available free of charge via the Internet at http://pubs.acs.org.

AUTHOR INFORMATION

Corresponding Author

*Tel: +82-2-880-4338. Fax: +82-2-875-6636. E-mail: dalheemin@snu.ac.kr.

Notes

The authors declare no competing financial interest.

ACKNOWLEDGMENTS

REFERENCES

(1) Yukihira, D.; Miura, D.; Saito, K.; Takahashi, K.; Wariishi, H. *Anal. Chem.* **2010**, *82*, 4278.

(2) Jungbauer, L. M.; Cavagnero, S. *Anal. Chem.* **2006**, *78*, 2841.

(3) Franck, J.; Arafah, K.; Elayed, M.; Bonnel, D.; Vergara, D.; Jacquet, A.; Vinatier, D.; Wisztorski, M.; Day, R.; Fournier, I.; Salzet, M. *Mol. Cell. Proteomics.* **2009**, *8*, 2023.

(4) Yates, J. R.; Ruse, C. I.; Nakorchevsky, A. *Annu. Rev. Biomed. Eng.* **2009**, *11*, 49.

(5) Liu, T.; Belov, M. E.; Jaitly, N.; Qian, W. J.; Smith, R. D. *Chem. Rev.* **2007**, *107*, 3621.

(6) Karas, M.; Hillenkamp, F. *Anal. Chem.* **1988**, *60*, 2299.

(7) Guo, Z.; Zhang, Q.; Zou, H.; Guo, B.; Ni, J. *Anal. Chem.* **2002**, *74*, 1637.

(8) Tholey, A.; Heinzle, E. *Anal. Bioanal. Chem.* **2006**, *386*, 24.

(9) Galesio, M.; Rial-Otero, R.; Capelo-Martínez, J. L. *Rapid Commun. Mass Spectrom.* **2009**, *23*, 1783.

(10) Wei, J.; Buriak, J. M.; Siuzdak, G. *Nature* **1999**, *399*, 243.

(11) Thomas, J. J.; Shen, Z.; Crowell, J. E.; Finn, M. G.; Siuzdak, G. *Proc. Natl. Acad. Sci. U. S. A.* **2001**, *98*, 4932.

(12) Lewis, W.; Shen, Z.; Finn, M. G.; Siuzdak, G. *Int. J. Mass Spectrom.* **2003**, *226*, 107.

(13) Chen, C. T.; Chen, Y. C. *Rapid Commun. Mass Spectrom.* **2004**, *18*, 1956.

(14) Wang, H.; Duan, J.; Cheng, Q. *Anal. Chem.* **2011**, *83*, 1624.

(15) Shenar, N.; Martinez, J.; Enjalbal, C. *J. Am. Soc. Mass Spectrom.* **2008**, *19*, 632.

(16) Duan, J.; Linman, M. J.; Cheng, Q. *Anal. Chem.* **2010**, *82*, 5088.

(17) Chen, L. C.; Yonehama, J.; Ueda, T.; Hori, H.; Hiraoka, K. *J. Mass Spectrom.* **2007**, *42*, 346.

(18) Liu, R.; Liu, J. F.; Zhou, X. X.; Jiang, G. B. *Anal. Chem.* **2011**, *83*, 3668.

(19) Kailasa, S. K.; Kiran, K.; Wu, H. F. *Anal. Chem.* **2008**, *80*, 9681.

(20) Shastri, L. A.; Kailasa, S. K.; Wu, H. F. *Rapid Commun. Mass Spectrom.* **2009**, *23*, 2247.

(21) Kailasa, S. K.; Wu, H. F. *Rapid Commun. Mass Spectrom.* **2011**, *25*, 271.

(22) Tanaka, K.; Waki, H.; Ido, Y.; Akita, S.; Yoshida, Y.; Yoshida, T. *Rapid Commun. Mass Spectrom.* **1988**, *2*, 151.

(23) McLean, J. A.; Stumpo, K. A.; Russell, D. H. *J. Am. Chem. Soc.* **2005**, *127*, 5304.

(24) Kawasaki, H.; Yonezawa, T.; Watanabe, T.; Arakawa, R. *J. Phys. Chem. C* **2007**, *111*, 16278.

(25) Sherrod, S. D.; Diaz, A. J.; Russell, W. K.; Cremer, P. S.; Russell, D. H. *Anal. Chem.* **2008**, *80*, 6796.

(26) Xu, S.; Li, Y.; Zou, H.; Qiu, J.; Guo, Z.; Guo, B. *Anal. Chem.* **2003**, *75*, 6191.

(27) Ren, S. F.; Guo, Y. L. *Rapid Commun. Mass Spectrom.* **2005**, *19*, 255.

(28) Ren, S. F.; Guo, Y. L. *J. Am. Soc. Mass Spectrom.* **2006**, *17*, 1023.

(29) Pan, C.; Xu, S.; Zou, H.; Guo, Z.; Zhang, Y.; Guo, B. *J. Am. Soc. Mass Spectrom.* **2005**, *16*, 263.

(30) Hen, W. Y.; Wang, L. S.; Chiu, H. T.; Chen, Y. C.; Lee, C. Y. *J. Am. Soc. Mass Spectrom.* **2004**, *15*, 629.

(31) Dong, X.; Cheng, J.; Li, J.; Wang, Y. *Anal. Chem.* **2010**, *82*, 6208.

(32) Zhou, X.; Wei, Y.; He, Q.; Boey, F.; Zhang, Q.; Zhang, H. *Chem. Commun.* **2010**, *46*, 6974.

(33) Tang, L.A.; Wang, J.; Loh, K. P. *J. Am. Chem. Soc.* **2010**, *132*, 10976.

(34) Gulbakan, B.; Yasun, E.; Shukoor, M. I.; Zhu, Z.; You, M.; Tan, X.; Sanchez, H.; Powell, D. H.; Dai, H.; Tan, W. *J. Am. Chem. Soc.* **2010**, *132*, 17408.

(35) Ren, S. F.; Zhang, L.; Cheng, Z. H.; Guo, Y. L. *J. Am. Soc. Mass Spectrom.* **2005**, *16*, 333.

(36) Lee, J.; Kim, Y. −K.; Min, D. −H. *J. Am. Chem. Soc.* **2010**, *132*, 14714.

2094

dx.doi.org/10.1021/am300054z | *ACS Appl. Mater. Interfaces* 2012, 4, 2088−2095

(37) Kim, Y. −K.; Na, H. −K.; Kwack, S. −J.; Ryoo, S. −R.; Lee, Y.; Hong, S.; Hong, S.; Jeong, Y.; Min, D. −H. *ACS Nano* **2011**, *5*, 4550.

(38) Decher, G.; Hong, J. −D. *Ber. Bunsen-Ges.* **1991**, *95*, 1430.

(39) Ariga, K.; Hill, J. P.; Ji, Q. *Phys. Chem. Chem. Phys.* **2007**, *9*, 2319.

(40) Smith, R. C.; Riollano, M.; Leung, A.; Hammond, P. T. *Angew. Chem. Int. Ed.* **2009**, *48*, 8974.

(41) Such, G. K.; Johnston, A. P.; Caruso, F. *Chem. Soc. Rev.* **2011**, *40*, 19.

(42) Lee, D. W.; Hong, T. −K.; Kang, D.; Lee, J.; Heo, M.; Kim, J. Y.; Kim, B. −S.; Shin, H. S. *J. Mater. Chem.* **2011**, *21*, 3438.

(43) Lee, S.W.; Yabuuchi, N.; Gallant, B.M.; Chen, S.; Kim, B. −S.; Hammond, P.T.; Yang, S. −H. *Nat. Nanotechnol.* **2010**, *5*, 531.

(44) Li, X.; Xu, W.; Zhang, J.; Jia, H.; Yang, B.; Zhao, B.; Li, B.; Ozaki, Y. *Langmuir* **2004**, *20*, 1298.

(45) Hu, X.; Cheng, W.; Wang, T.; Wang, Y.; Wang, E.; Dong, S. *J. Phys. Chem. B.* **2005**, *109*, 19385.

(46) Kawasaki, H.; Sugitani, T.; Watanabe, T.; Yonezawa, T.; Moriwaki, H.; Arakawa, R. *Anal. Chem.* **2008**, *80*, 7524.

(47) Li, D.; Müller, M. B.; Gilje, S.; Kaner, R. B.; Wallace, G. G. *Nat. Nanotechnol.* **2008**, *3*, 101.

(48) Lee, S. W.; Kim, B.-S.; Chen, S.; Yang, S.-H.; Hammond, P. T. *J. Am. Chem. Soc.* **2009**, *131*, 671.

(49) Ramanathan, T.; Fisher, F. T.; Ruoff, R. S.; Brinson, L. C. *Chem. Mater.* **2005**, *17*, 1290.

(50) Hummers, W. S.; Offeman, R. E. *J. Am. Chem. Soc.* **1958**, *80*, 1339.

(51) Kim, Y. −K.; Min, D. −H. *Langmuir* **2009**, *25*, 11302.

(52) Tang, H. W.; Ng, K. M.; Lu, W.; Che, C. M. *Anal. Chem.* **2009**, *81*, 4720.

(53) van Meer, G.; Voelker, D. R.; Feigenson, G. W. *Nat. Rev. Mol. Cell Biol.* **2008**, *9*, 112.